Production of π^+ and K^+ mesons in 3.2 AGeV argon-nucleus interactions at the Nuclotron

BM@N Collaboration

Abstract

The BM@N (Baryonic Matter at Nuclotron) is the first experiment undertaken at the accelerator complex of NICA-Nuclotron. The BM@N scientific program comprises studies of dense nuclear matter in heavy ion beams of the intermediate energy range between the SIS-18 and NICA/FAIR facilities. The experimental run was performed in the argon beam of the 3.2 AGeV kinetic energy with fixed targets. First physics results are presented on π^+ and K^+ meson production in argon-nucleus interactions. Transverse momentum, rapidity spectra and yields of π^+ and K^+ mesons are measured. The results are compared with predictions of theoretical models.

1 Introduction

Collisions of relativistic heavy ions provide a unique opportunity to study nuclear matter at extreme densities and temperatures. At the Nuclotron, the experimental research is focused on studies of hadrons with strangeness produced in the collision and not present in the initial state of two colliding nuclei, unlike the nucleons consisting of light (*u* and *d*) quarks. The energy range of ion beams at the Nuclotron corresponds to $\sqrt{s_{NN}} = 2.3 - 3.5$ GeV. At the Nuclotron energies the nucleon density in a fireball created by two colliding heavy nuclei is 3-4 times higher than the saturation density [1]. In addition, these energies are high enough to study strange mesons and (multi)-strange hyperons produced in nucleus-nucleus collisions close to the kinematic threshold [2, 3].

BM@N (Baryonic Matter at Nuclotron) is the first experiment operational at the Nuclotron/ NICA accelerating complex. The purpose of the BM@N experiment is to study relativistic heavy ion beam interactions with fixed targets [7] in the energy range of maximal baryon densities [4]. The primary goal is to constrain parameters of the Equation of State of high density nuclear matter. Studies of the excitation function of strange particle production below and close to the kinematical threshold provide the means to differentiate hard from soft behaviour of EoS [5]. The Nuclotron will provide the experiment with beams of a variety of particles, from protons to gold ions, with a kinetic energy ranging from 1 to 6 GeV/nucleon for light ions with Z/A ratio of 0.5 and up to 4.5 GeV/nucleon for heavy ions with Z/A ratio of 0.4. Recently BM@N collected first experimental data in beams of carbon, argon, and krypton ions [8, 9]. This paper presents first results on π^+ and K^+ meson production in argon-nucleus interactions. Transverse momentum, rapidity spectra and yields of π^+ and K^+ mesons are measured. The results are compared with predictions of theoretical models and with the experimental data on middle size nucleus-nucleus interactions measured at lower energies.

2 Experimental set-up

The experimental run of the BM@N detector was performed with the argon beam in 2018. The view of the BM@N setup used in the run is presented in Fig. 1. The experimental data from a central tracker, outer drift chambers (DCH), a cathode strip chamber (CSC), time-of-flight detectors (ToF), zero degree calorimeter (ZDC), trigger and T0 detectors (T0T) were read out using the integrated data acquisition system. The configuration of the central tracker was based on three planes of double-side forward silicon detectors (Si) with the maximal size of 25x25 cm^2 situated behind the target and six two-coordinate GEM (Gaseous Electron Multiplier) detectors with the size of 163x45 cm^2 [6] situated at distances from 40 to 240 cm from the target. The tracking stations were arranged to cover the upper part of the acceptance of the analyzing magnet, so that the beam passed through the arcway at the bottom side of the GEM detectors. The positions of the silicon and GEM detectors within the analysing magnet are shown in Fig. 2. Each successive GEM detector was rotated by 180^o around the vertical axis. It was done to have the opposite electron drift direction in the successive detectors in order to avoid a systematic shift of reconstructed tracks due to the Lorentz angle in the magnetic field. Experimental data of beam interactions with different targets were analyzed with the aim to reconstruct tracks, primary and secondary vertices using the central tracking detectors. The research program was devoted to measurements of inelastic reactions $Ar + A \to X$ with the beam kinetic energy of 3.2 AGeV and different targets: C, Al, Cu, Sn, Pb.

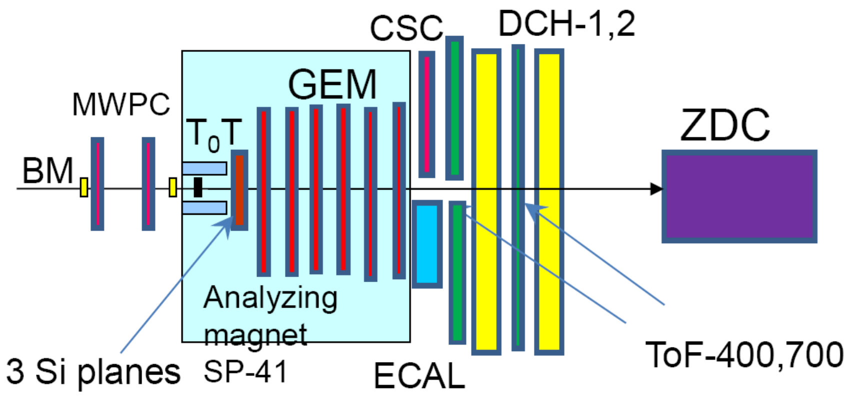

Figure 1: Scheme of the BM@N set-up in the argon beam run.

The argon beam intensity was few 10^5 per the spill, the spill duration was 2-2.5 sec. In the present analysis the experimental data from the forward silicon detectors, GEM detectors, outer drift chambers, cathode strip chamber and two sets of the time-of-flight detectors ToF-400 and ToF-700 were used. The magnetic field in the center of the analyzing magnet was 0.61 T. To form a trigger signal, different conditions were required on the minimum number of fired channels in the barrel BD detector situated around the target and the multiplicity silicon FD trigger detector behind the target, ranging from zero to 4 for different runs. The data samples included “good quality” runs where the CSC (DCH) and ToF-400 (ToF-

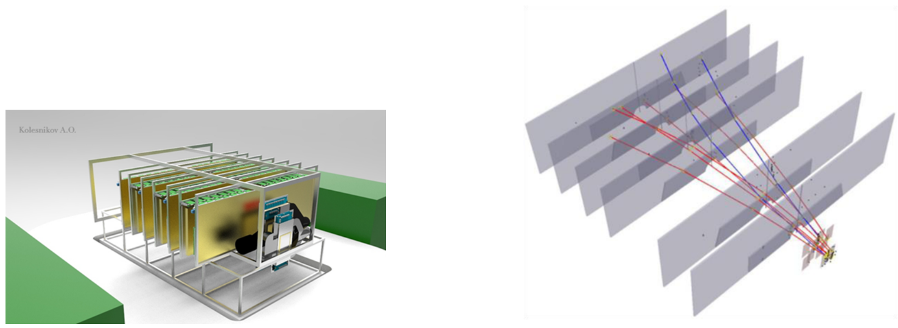

Figure 2: Left: Scematic view of the central tracking system consisting of the silicon strip and GEM detectors. Right: Argon-nucleus interaction reconstructed in the central tracking system based on the silicon and GEM detectors.

700) detectors were fully operational. The analysed statistics of argon-nucleus collisions was 83M events for 3.2 AGeV argon beam data.

3 Event reconstruction

The track reconstruction method was based on the so-called 'cellular automaton' approach [10] . π^+ and K^+ mesons were identified using the time of flight measured in T0 and ToF detectors, the length of the trajectory and the momentum reconstructed in the central tracker. Candidates to π^+ and K^+ should originate from the primary event vertex, correlate with hits in the CSC / DCH detectors and match hits in the ToF-400 / ToF-700 detectors. Herewith, the CSC / DCH hits were used to confirm the quality of the tracks matched to ToF-400 /ToF-700 hits. The criteria for selection of π^+ and K^+ meson candidates were the following:

- Each track has at least 4 hits in the GEM detectors (6 detectors in total), where a hit is a combination of two strip clusters on both readout sides (vertical X strips and X' strips at $\pm 15^o$ to the X strips) on each detector [6];

- Tracks are originated from the primary event vertex, the deviation of the reconstructed vertex from the position of the target along the beam direction -3.4 cm $< Z_{ver} - Z_0 <$ 1.7 cm, where Z_0 is the target position. The upper limit corresponds to 7σ of the Z_{ver} spread and cuts off interactions with the trigger detector behind the target;

- Distance from a track to the primary event vertex in the X-Y plane at Z_{ver} is required to be less than 1 cm;

- Momentum range of positive tracks $p > 0.5, 0.7$ GeV/c is limited by the acceptance of the ToF-400 and ToF-700 detectors, respectively;

- Distance of extrapolated tracks to the CSC / DCH hits as well as to the ToF-400 / ToF-700 hits should be within $\pm 2.5\sigma$ of the hit-track residual distributions.

Spectra of the mass squared of identified positive particles produced in interactions of the 3.2 AGeV argon beam with different targets are shown in Fig.3 for ToF-400 and ToF-700 data. Signals of π^+ and K^+ were extracted in windows of the mass squared from -0.09 to 0.13 (GeV/c^2)^2 and from 0.18 to 0.32 (GeV/c^2)^2, respectively. Numbers of π^+ and K^+ were taken from the content of the histogram bins within the corresponding mass windows. The errors of the π^+ and K^+ signals include the uncertainty of the background subtraction. The π^+ and K^+ signals, statistical errors were calculated according to the formulae: $sig = hist - bg$, $err_{stat} = \sqrt{hist + bg}$, assuming the background uncertainty of $\sqrt{bg}$. Here $hist$ and bg denote the histogram integral and the background integral within the π^+ and K^+ mass squared windows. To estimate the background in the π^+ and K^+ mass squared windows, the "mixed event" method was used, i.e. the shape of the mass squared background distribution was evaluated by matching tracks to hits in the ToF-400 and ToF-700 detectors originated from independent events. Signals of π^+ and K^+ in the intervals of the transverse momentum p_T and rapidity y in the laboratory frame were reconstructed using the same procedure. To estimate the π^+ and K^+ signal sistematic errors due to the background subtraction method, the distributions were fitted to the 1st degree polynomial (linear fit) in the mass squared range -0.14-0.4 (GeV/c^2)^2. The π^+ and K^+ mass squared windows were excluded from the linear fit. The variation of the background integral in the π^+ (K^+) mass squared window taken from mixed events relative to the bg integral taken from the fit of the mass squared spectra was treated as a systematic error.

4 Reconstruction efficiency

Monte Carlo event samples of argon-nucleus collisions were produced with the DCM-SMM event generator [11, 12]. The passage of particles through the setup volume was simulated with the GEANT3 program [13] integrated into the BmnRoot software framework [14]. To properly describe the GEM detector response in the magnetic field, the micro-simulation package Garfield++ [15] was used.

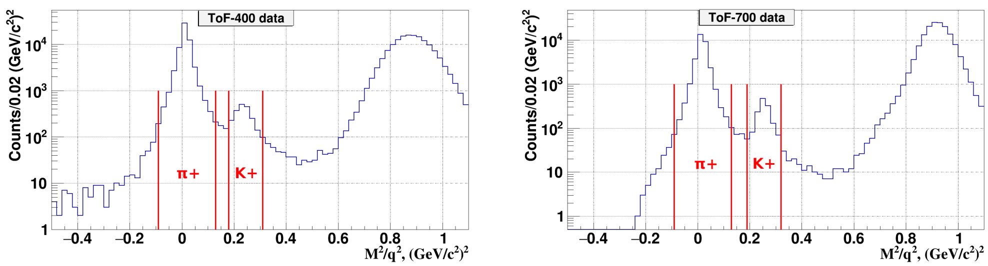

Figure 3: Mass squared spectra of identified positive particles produced in argon-nucleus interactions and measured in the ToF-400 (left plot) and ToF-700 detectors (right plot).

The package gives very detailed description of the processes inside the GEM detector, including the drift and diffusion of released electrons in electric and magnetic fields and the electron multiplication in GEM foils, so that the output signal from the readout plane can be reproduced. The details of the detector alignment, Lorentz shift corrections are described in the paper [16].

The efficiencies of the forward silicon, GEM, CSC, DCH and ToF detectors were adjusted in simulation to the detector efficiencies measued in experimental events. The resulting π^+ and K^+ reconstruction efficiency is the ratio of the number of reconstructed π^+ and K^+ mesons to the number of generated ones in the intervals of (y, p_T), where y is measured in the laboratory frame. The reconstruction efficiency is a product of the geometrical acceptance, detector efficiency and efficiency of kinematic and spatial cuts. The obtained values of the π^+ and K^+ reconstruction efficiency are shown in Fig. 4 in the y and p_T intervals for Ar+Cu interactions.

Different conditions were applied on the minimum number of fired channels in the barrel BD and multiplicity silicon FD trigger detectors, ranging from zero to 4, to record experimental data. The efficiency to get a trigger signal based on multiplicities of fired channels in the BD (FD) detectors ϵ_{trig} was calculated for events with reconstructed π^+ and K^+ using experimental event samples recorded with an independent trigger based on the FD (BD) detectors: ϵ_{trig} (BD $\geq$ m) = N(BD $\geq$ m, FD $\geq$ n)/ N(FD $\geq$ n). The dependences of trigger efficiency on the track multiplicity from the primary event vertex and the vertex position were taken into account. The efficiency for the combined BD and FD triggers was calculated as a product of the BD and FD trigger efficiencies. The systematic errors used in the analysis cover the differences in the $\pi+$, K^+ signals obtained by using the

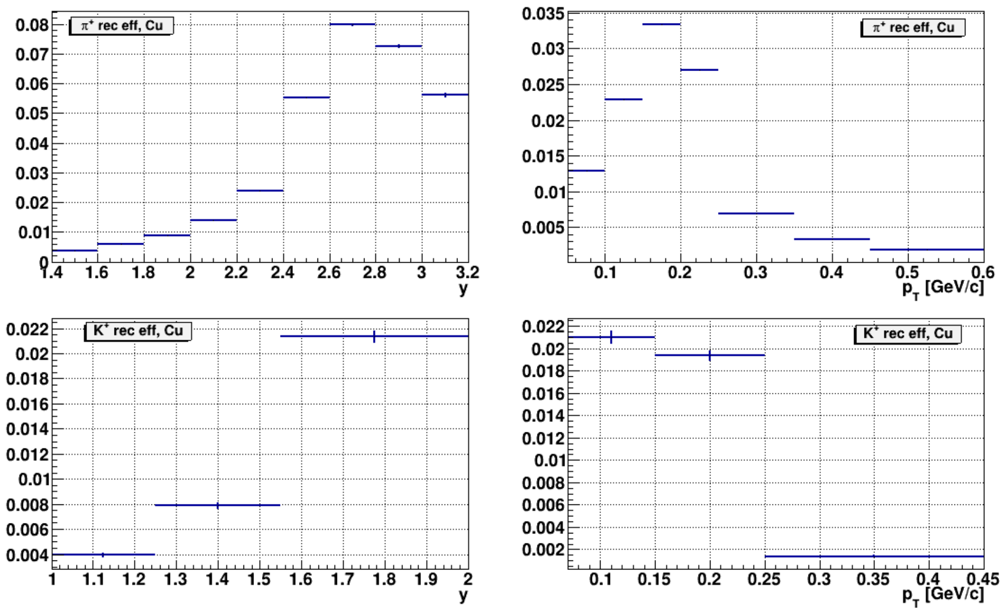

Figure 4: Reconstruction efficiency of π^+ and K^+ calculated as a product of the geometrical acceptance, detector efficiency and efficiency of kinematic and spatial cuts in bins of rapidity y in the laboratory frame and in bins of p_T. Results are shown for Ar+Cu interactions at the 3.2 AGeV argon beam energy.

mean values of the trigger efficiency values instead of the efficiency dependences on the number of the vertex tracks and the primary vertex position.

5 Results

The inclusive cross sections $\sigma_{\pi,K}$ and yields $Y_{\pi,K}$ of π^+ and K^+ meson production in Ar+C, Al, Cu, Sn, Pb interactions are calculated in bins of $y(\,p_T)$ according to the formulae:

$$\sigma_{\pi,K}(y,p_T) = N_{\pi,K}(y,p_T)/(\epsilon_{rec}(y,p_T)\cdot\epsilon_{trig}\cdot L), Y_{\pi,K}(y,p_T) = \sigma_{\pi,K}(y,p_T)/\sigma_{inel}$$

where L is the luminosity, $N_{\pi,K}$ is the number of reconstructed π^+ and K^+ mesons, ϵ_{rec} is the efficiency of the π^+ and K^+ meson reconstruction, ϵ_{trig} is the trigger efficiency, σ_{inel} is the cross section for minimum bias inelastic argon-nucleus interactions. The cross sections for inelastic Ar+C, Al, Cu, Sn, Pb interactions are taken from the predictions of the DCM-SMM model which are consistent with the results calculated by the formula: $\sigma_{inel} = \pi R_0^2(A_P^{1/3} + A_T^{1/3})^2$, where $R_0 = 1.2$ fm is an effective nucleon radius, A_P and A_T are atomic numbers of the projectile and target nucleus [28]. The uncertainties for Ar+C, Al, Cu, Sn, Pb inelastic cross sections are estimated from the alternative formula: $\sigma_{inel} = \pi R_0^2 (A_P^{1/3} + A_T^{1/3} - b)^2$ with $R_0 = 1.46$ fm and $b = 1.21$ [19]. The values and uncertainties of σ_{inel} for Ar+C, Al, Cu, Sn, Pb interactions used to evaluate the π^+ and K^+ meson yields are given in Table 1.

The yields of π^+ (K^+) mesons in Ar+C, Al, Cu, Sn, Pb interactions are measured in the kinematic range of the π^+ (K^+) meson transverse momentum $0.1 < p_T < 0.6$ GeV/c ($0.1 < p_T < 0.5$ GeV/c) and the π^+ (K^+) meson rapidity in the laboratory frame $1.5 < y < 3.2$ ($1.0 < y < 2.0$). The systematic error of the π^+ and K^+ meson yield in every p_T and y bin is calculated as a quadratic sum of uncertainties coming from the following sources:

- Systematic errors of the reconstruction efficiency due to the remaining difference in the X/Y primary vertex distribution in the simulation relative to the experimental data.

- Systematic errors of the background subtraction under the π^+ and K^+ signals in the mass squared spectra of identified particles as described in section 3.

- Systematic error of the trigger efficiency evaluated as a function of the number of tracks from the primary vertex and the primary vertex position.

The π^+ and K^+ meson yield normalization uncertainties are calculated for the whole measured (y, p_T) range as a quadratic sum of the statistical uncertainty of the trigger efficiency, uncertainties of the tracking detector efficiency, efficiency of matching to the CSC (DCH) outer detectors and to ToF-400 (ToF-700), luminosity and inelastic nucleus-nucleus cross section. The luminosity uncertainty is estimated to be within 2%. The statistical uncertainty of the trigger efficiency is 28% for K^+ detection in Ar+C interactions and between 7.5% (Ar+Al) and 4% (Ar+Pb) for K^+ detection in interactions of argon with heavier targets. The trigger efficiency uncertainty for π^+ detection ranges between 4.5% (Ar+C) and 0.9% (Ar+Pb). The uncertainty of the central tracking detector efficiency is estimated to be within 3%. The uncertainty of matching of extrapolated tracks with the CSC (DCH) hits as well as with the ToF-400 (ToF-700) hits is within 5%.

The rapidity of the beam-target nucleon-nucleon CM system calculated for an interaction of the argon beam with the kinetic energy of 3.2 GeV/nucleon with a fixed target is $y_{CM} = 1.08$. The transformation of the y distribution from the laboratory to the CM system gives $y^* = y - y_{CM}$. The differential y spectra of the π^+ and K^+ meson yields corrected for the detector acceptance and efficiency are measured in p_T bins and presented in Fig. 5 and 6, respectively. The predictions of the DCM-SMM [11, 12], UrQMD [17] and PHSD [18] models are shown for comparison. Although the DCM-SMM model was used to evaluated the reconstrucion efficiency (section 4) the model predictions could differ from the measurement results. The corrected differential invariant p_T spectra of π^+ and K^+ meson yields are measured in bins of rapidity y and presented in Fig. 7 and 8, respectively. Due to low statistics of the K^+ meson signal in Ar+C interac tions, the results are given only for the whole measured range in y and p_T. The invariant p_T spectra of K^+ meson yields in the whole measured rapidity range are presented in Fig. 9 (optional Fig.). In Fig. 7, 8 and 9 the measured invariant p_T spectra of the π^+ and K^+ meson yields are parameterized by the form: $1/p_T d^2N/dp_T dy \propto \exp(-(m_T - m_{\pi,K})/T_0)$, where $m_T = \sqrt{m_{\pi,K}^2 + p_T^2}$ is the transverse mass, the inverse slope parameter T_0 is a free parameter of the fit, dy is the width of the measured y bin. The values of the inverse slope T_0, extracted from the fits to the invariant p_T spectra of π^+ and K^+ mesons are given in Fig. 10 and 11, respectively. The value of T_0 measured for pi^+ mesons in argon-nucleus interactions at the beam kinetic energy of 3.2 AGeV is about 40 MeV in the forward rapidity range rising up 90 MeV in the central rapidity range. The y dependence of the fit results for π^+ mesons are consistent with predictions of the DCM-SMM, UrQMD and PHSD models. In general, the considered transport models describe the shape of the differential spectra on y and p_T, but predict more abundant yields of π^+ and K^+ mesons in Ar+C interactions than measured in the experiment. There is a tendency that the BM@N measures a flatter dependence of the T_0 values in the π^+ central rapidity range compared with the models. The T_0 slope values measured in 3 y bins for K^+ mesons have rather large statistical and systematic errors (see Fig. 11), but the T_0 values obtained for the whole measured $1.0 < y < 2.0$ range are consistent within the errors with 80 MeV for all the targets (see Table 1). The ratios of K^+ to π^+ yields also given in Table 1 show no visible dependence on the atomic weight of the target.

The measured yields of π^+ and K^+ mesons in Ar+C, Al, Cu, Sn, Pb interactions are extrapolated to the full kinematic range using predictions of the DCM-SMM model. The π^+ and K^+ meson yields and cross sections in Ar+C, Al, Cu, Sn, Pb interactions are summarized in Table 1. The BM@N results are compared with the predictions of the DCM-SMM, UrQMD and PHSD models.

The π^+ and K^+ meson yields in argon-nucleus interactions can be compared with the previous results of the HADES experiment measured at the lower beam kinetic enegy of 1.76 AGeV in Ar+KCl interations [20–22] and with the measure ments of the FOPI experiment in Ni+Ni interacions at the beam kinetic energy 1.93 AGeV [23–25]. The KaoS experiment also measured K^+ yields in Ni+Ni interactions at 1.5 and 1.93 AGeV [26, 27] consistent with the results of the FOPI experiment. The HADES experiment measured the total multiplicities of π^- and K^+ in cemi-central events (the mean number of nucleons - participants $\langle Apart \rangle$ of 38.5) of 3.9 and $2.8 \cdot 10^{-2}$, respectively. The effective inverse slope parameters of the m_T spectra of π^- and K^+ extrapolated to $y^* = 0$ are 82.4 MeV and 89 MeV, respectively. The BM@N results on the K^+ and π^+ multiplicities at the beam kinetic energy of 3.2 AGeV in Ar+Al interactions ($\langle Apart \rangle \sim (A_P + A_T)/2$ of 33.5) (see Table 1) are higher by a factor 3.5 for kaons and comparable in values for pions withe the HADES measurements. The inverse slope parameters T_0 measured for π^+ and K^+ in the central rapidity range (see Figures 10 and 10) are comparable with the results of HADES.

The FOPI experiment measured the total multiplicities of K^+ in triggered semi-central Ni+Ni interactions (themean number of nucleons - participants $\langle A_{part} \rangle$ of 46.5) and central events ($\langle A_{part} \rangle$ of 75) of $3.6 \cdot 10^{-2}$ and $8.5 \cdot 10^{-2}$, respectively. These values could be compared with the BM@N results presented in Table 1 for different targets. The K^+/π^+ ratio measured by FOPI in triggered semi-central events is $7.6 \cdot 10^{-3}$, which is a factor 3 smaller of the K^+/π^+ ratio obtained by BM@N in Ar + Sn interactions for the full kinematical range ($\langle A_{part} \rangle$ of 52) (see Table 1). The effective inverse slope of 110.9 MeV for the K^+ transverse mass spectrum evaluated by FOPI at $y^* = 0$ is consistent within the uncertainies with the inverse slope parameter T_0 measured by BM@N for K^+ in the range $y^* \geq 0$.

6 Summary

First physics results of the BM@N experiment are presented on the π^+ and K^+ meson yields and their ratios in argon-nucleus interactions at the beam kinetic energies of 3.2 AGeV. The results are compared with models of nucleus-nucleus interactions and with the results of other experiments studied argon-nucleus interactions at lower energies.

Acknowledgments. The BM@N Collaboration acknowledges support of the HybriLIT of JINR, HPC Village project and HGPU group for the computational resources provided. This work is supported by the Russian Foundation for Basic Research (RFBR) under grant No. 18-02-40036 mega.

References

[1] B. Friman, W. Nörenberg, and V.D. Toneev, Eur. Phys. J. A **3** (1998).

[2] NICA White Paper, Eur.Phys.J. A52 (2016).

[3] BM@N Conceptual Design Report:
http://nica.jinr.ru/files/BM@N/BMN_CDR.pdf

[4] J. Randrup and J. Cleymans, Phys.Rev.C 74 (2006) 047901.

[5] Ch. Fuchs, Prog.Part.Nucl.Phys. 56 (2006) 1-103.

[6] D. Baranov et al., JINST 12 (2017) no.06, C06041.

[7] M. Kapishin (for the BM@N Collaboration), Eur.Phys.J. A52 (2016) no.8, 213.

[8] M. Kapishin (for the BM@N Collaboration), Nucl.Phys. A982 (2019) 967-970.

[9] M. Kapishin (for the BM@N Collaboration), SQM 2019 proceedings, 285 Springer Proc.Phys. 250 (2020) 21-27.

[10] V. Akishina and I. Kisel, J. Phys.: Conf. Ser. 599, 012024 (2015), I. Kisel, Nucl. Instrum. Meth. A **566**, 85 (2006).

[11] N. Amelin, K. Gudima, and V. Toneev, Sov.J.Nucl. Phys. 51, 1093 (1990).

[12] M. Baznat, A. Botvina, G. Musulmanbekov, V. Toneev, V. Zhezher, Phys.Part.Nucl.Lett. 17 (2020) no.3; arXiv: 1912.09277v.

[13] CERN Program Library, Long Writeup W5013, Geneva, CERN, 1993.

[14] https://git.jinr.ru/nica/bmnroot

[15] http://garfieldpp.web.cern.ch/garfieldpp

[16] D. Baranov et al., Phys.Part.Nucl.Lett. 15 (2018) no.2, 148-156.

[17] S.A. Bass *et al.*, Prog. Part. Nucl. Phys. 41 225 (1998).

[18] W. Cassing a and E.L. Bratkovskaya, Nucl.Phys.A 831 (2009) 215-242.

[19] H. Angelov et al., P1-80-473, JINR, Dubna.

[20] G. Agakishiev et al., HADES Collaboration, Eur.Phys.J.A 47 (2011) 21.

[21] G. Agakishiev et al., HADES Collaboration, Phys.Rev.C 80 (2009) 025209.

[22] G. Agakishiev et al., HADES Collaboration, Phys.Rev.C 82 (2010) 044907

[23] D. Best et al., FOPI Collaboration, Nucl.Phys.A 625 (1997) 307-324

[24] N. Bastid et al., FOPI Collaboration, Phys.Rev.C 76 (2007) 024906

[25] K. Piasecki et al., FOPI Collaboration, Phys.Rev.C 99 (2019) 1, 014904.

[26] M.Menzel et al., KaoS Collaboration, Phys.Lett.B 495 (2000) 26-32.

[27] A.Forster et al., KaoS Collaboration, Phys.Rev.C 75 (2007) 024906.

[28] K. Kanaki, PhD Thesis, Technische Universit$\ddot{a}$t Dresden, 2007.

Table 1: π^+ and K^+ meson yields measured in Ar+C, Al, Cu, Sn, Pb interactions at the argon beam energy of 3.2 AGeV. The first error given is statistical, the second error is systematic.

3.2 AGeV argon beam	Ar+C	Ar+Al	Ar+Cu	Ar+Sn	Ar+Pb
Measured π^+ yield	$0.275 \pm 0.006 \pm 0.027$	$1.00 \pm 0.01 \pm 0.07$	$1.14 \pm 0.01 \pm 0.08$	$1.28 \pm 0.01 \pm 0.09$	$1.25 \pm 0.01 \pm 0.08$
Full π^+ yield N_π	$0.943 \pm 0.019 \pm 0.092$	$3.86 \pm 0.04 \pm 0.27$	$5.15 \pm 0.05 \pm 0.35$	$6.35 \pm 0.05 \pm 0.44$	$7.03 \pm 0.07 \pm 0.48$
Measured K^+ yield$/10^{-2}$	$0.94 \pm 0.18 \pm 0.35$	$3.90 \pm 0.28 \pm 0.61$	$4.17 \pm 0.21 \pm 0.66$	$5.60 \pm 0.22 \pm 0.75$	$5.10 \pm 0.22 \pm 0.92$
Full K^+ yield $N_{K+}/10^{-2}$	$2.19 \pm 0.42 \pm 0.81$	$9.8 \pm 0.7 \pm 1.5$	$11.9 \pm 0.6 \pm 1.9$	$18.0 \pm 0.7 \pm 2.4$	$18.8 \pm 0.8 \pm 3.4$
$N_{K+}/N_{\pi+}/10^{-2}$ Measured range	$3.43 \pm 0.66 \pm 1.25$	$3.90 \pm 0.28 \pm 0.55$	$3.66 \pm 0.19 \pm 0.53$	$4.39 \pm 0.18 \pm 0.51$	$4.11 \pm 0.18 \pm 0.68$
$N_{K+}/N_{\pi+}/10^{-2}$ Full kin. range	$2.33 \pm 0.45 \pm 0.85$	$2.53 \pm 0.18 \pm 0.35$	$2.30 \pm 0.12 \pm 0.33$	$2.83 \pm 0.12 \pm 0.33$	$2.68 \pm 0.12 \pm 0.44$
K^+ inverse slope T_0, MeV measured range	$73 \pm 14 \pm 13$	$80 \pm 7 \pm 5$	$81 \pm 5 \pm 5$	$81 \pm 5 \pm 4$	$78 \pm 5 \pm 4$
σ_{inel}, mb	1470 ± 50 [28]	1860 ± 50 [28]	2480 ± 50 [28]	3140 ± 50 [28]	3940 ± 50 [28]

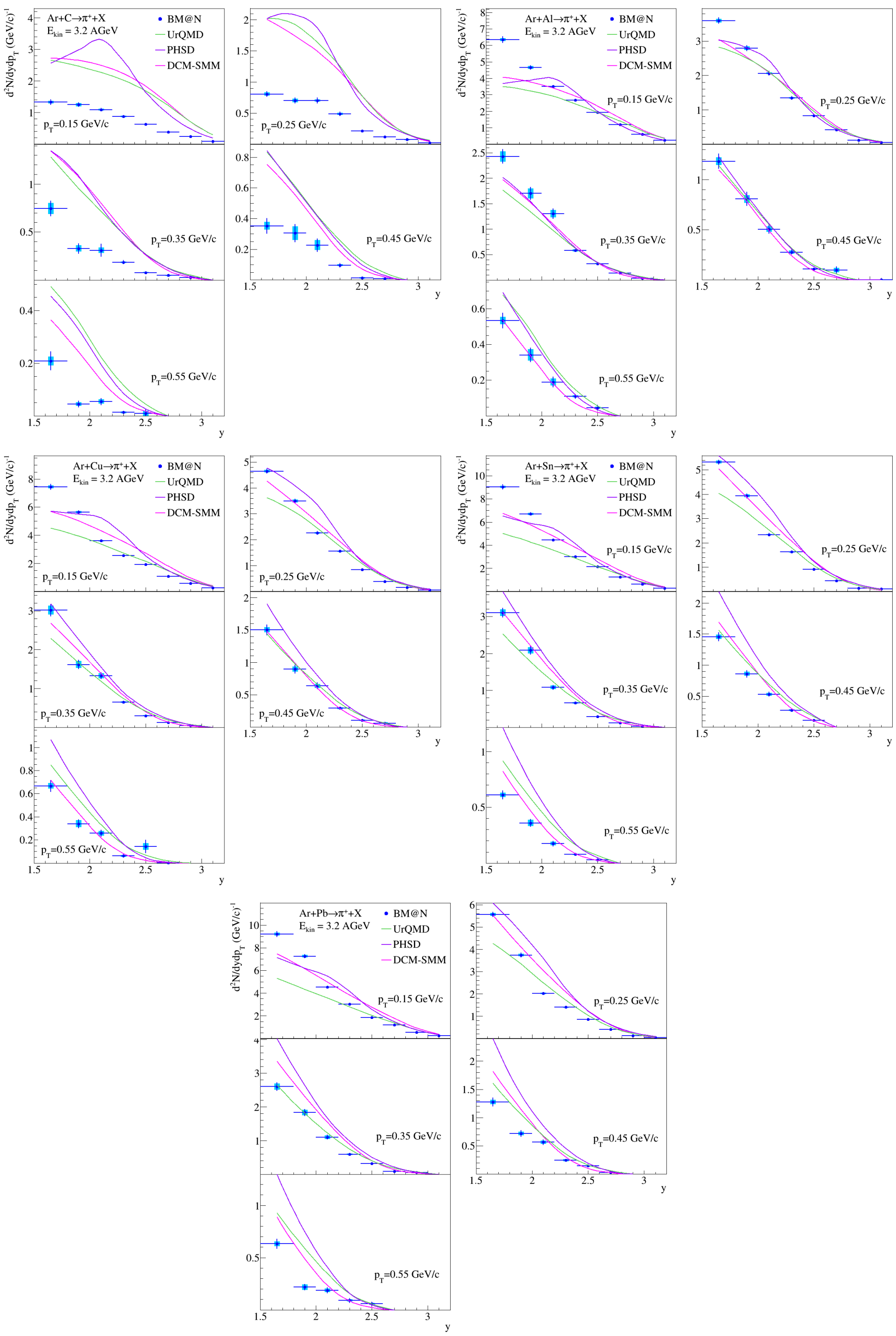

Figure 5: Rapidity y spectra of π^+ mesons produced in Ar+C, Al, Cu, Sn, Pb interactions at the argon beam energy of 3.2 AGeV. Results are given for bins of π^+ meson transverse momentum. The error bars represent the statistical errors, the boxes show the systematic errors. The predictions of the DCM-SMM, UrQMD and PHSD models are shown as rose, green and magenta lines.

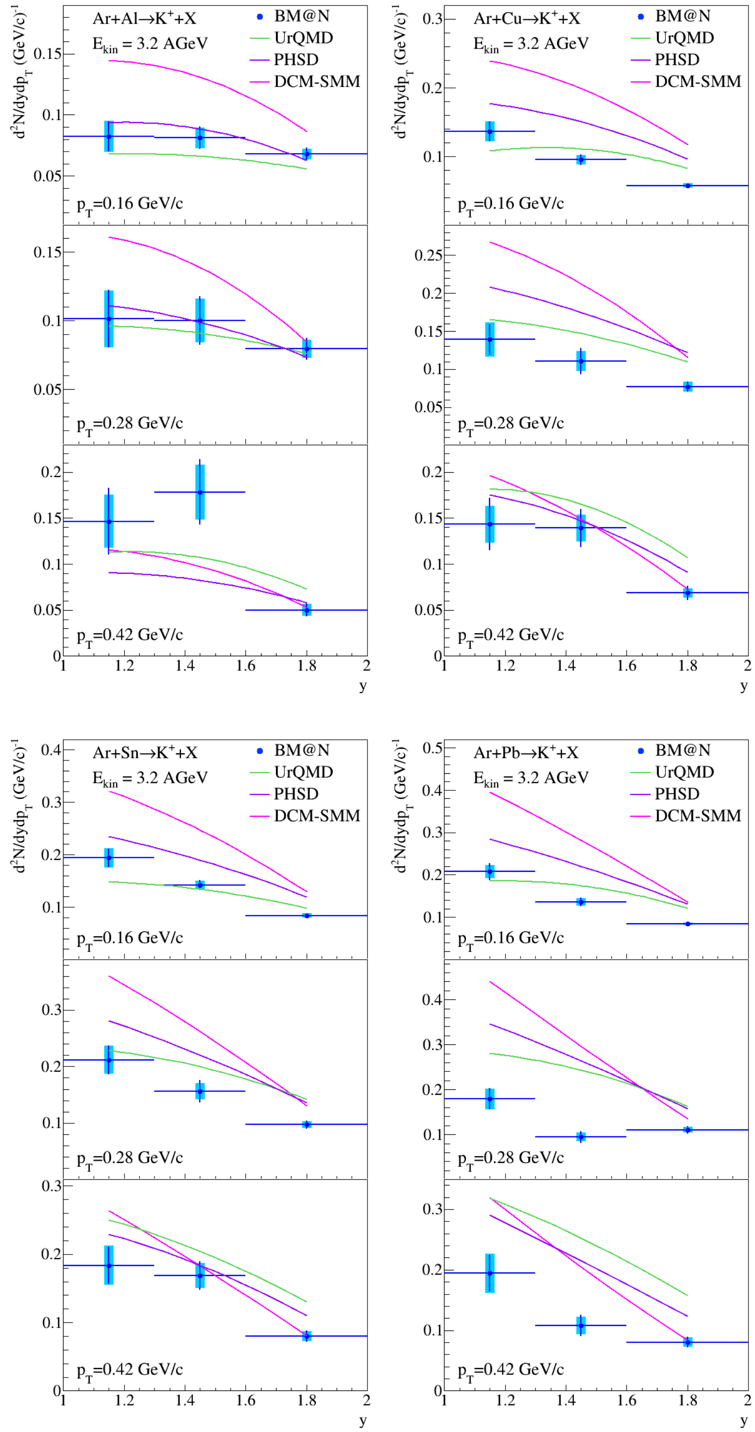

Figure 6: Rapidity y spectra of K^+ mesons produced in Ar+Al, Cu, Sn, Pb interactions at the argon beam energy of 3.2 AGeV. Results are given for bins of K^+ meson transverse momentum. The error bars represent the statistical errors, the boxes show the systematic errors. The predictions of the DCM-SMM, UrQMD and PHSD models are shown as rose, green and magenta lines.

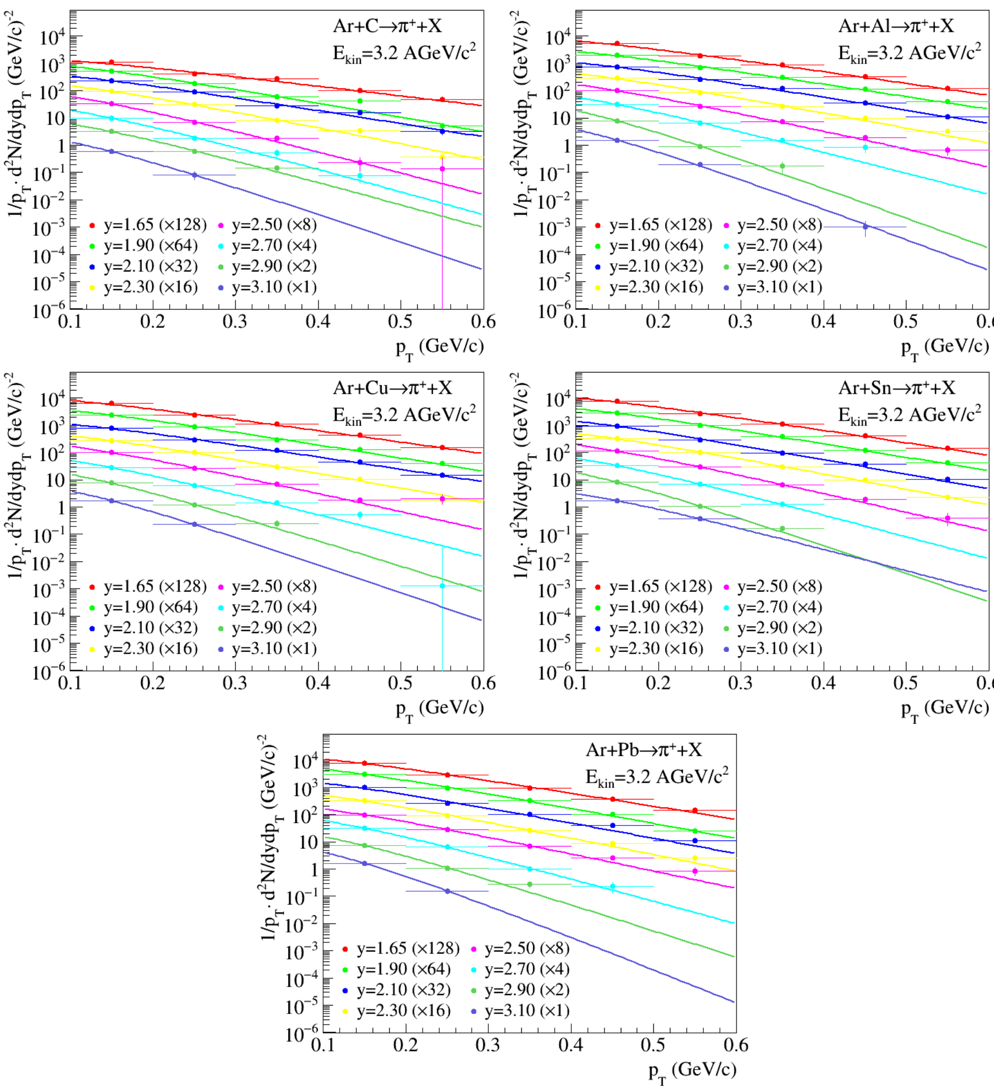

Figure 7: Invariant transverse momentum p_T spectra of π^+ mesons produced in Ar+C, Al, Cu, Sn, Pb interactions at the argon beam energy of 3.2 AGeV. Results are given for bins of π^+ meson rapidity. The lines represent the results of the parameterization described in the text.

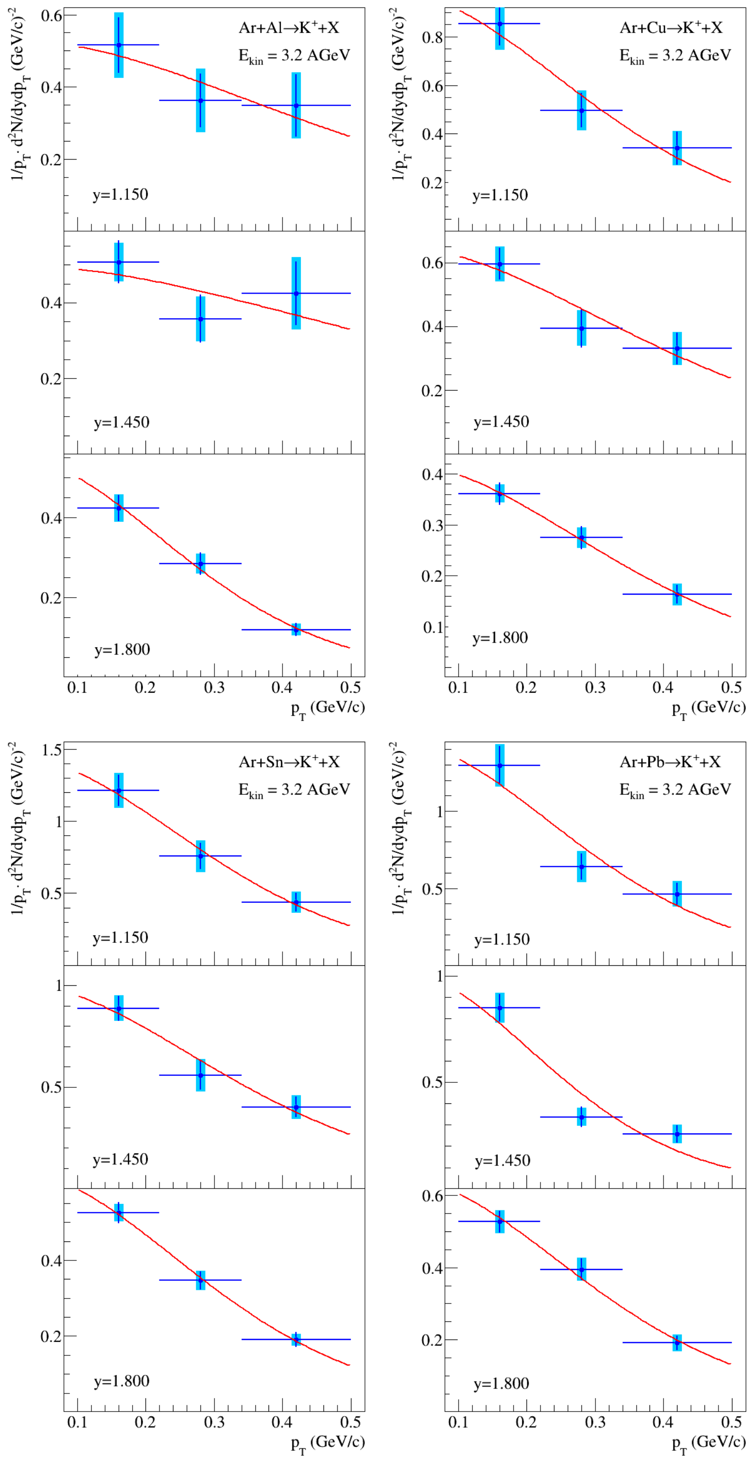

Figure 8: Invariant transverse momentum p_T spectra of K^+ mesons produced in Ar+C, Al, Cu, Sn, Pb interactions at the argon beam energy of 3.2 AGeV. Results are given for three bins of K^+ meson rapidity. The error bars represent the statistical errors, the boxes show the systematic errors. The lines represent the results of the parameterization described in the text.

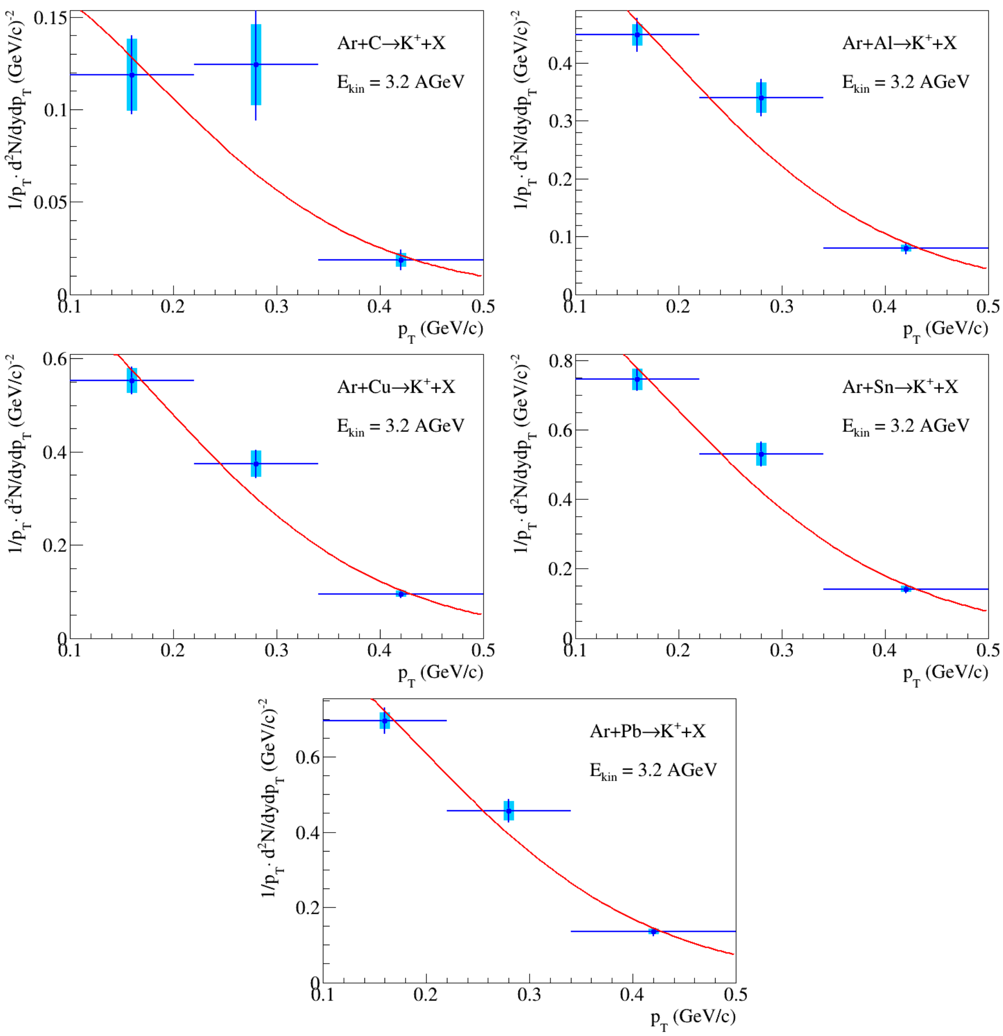

Figure 9: Invariant transverse momentum p_T spectra of K^+ mesons produced in Ar+C, Al, Cu, Sn, Pb interactions at the argon beam energy of 3.2 AGeV. Results are given for the measured K^+ meson rapidity range. The error bars represent the statistical errors, the boxes show the systematic errors. The lines represent the results of the parameterization described in the text.

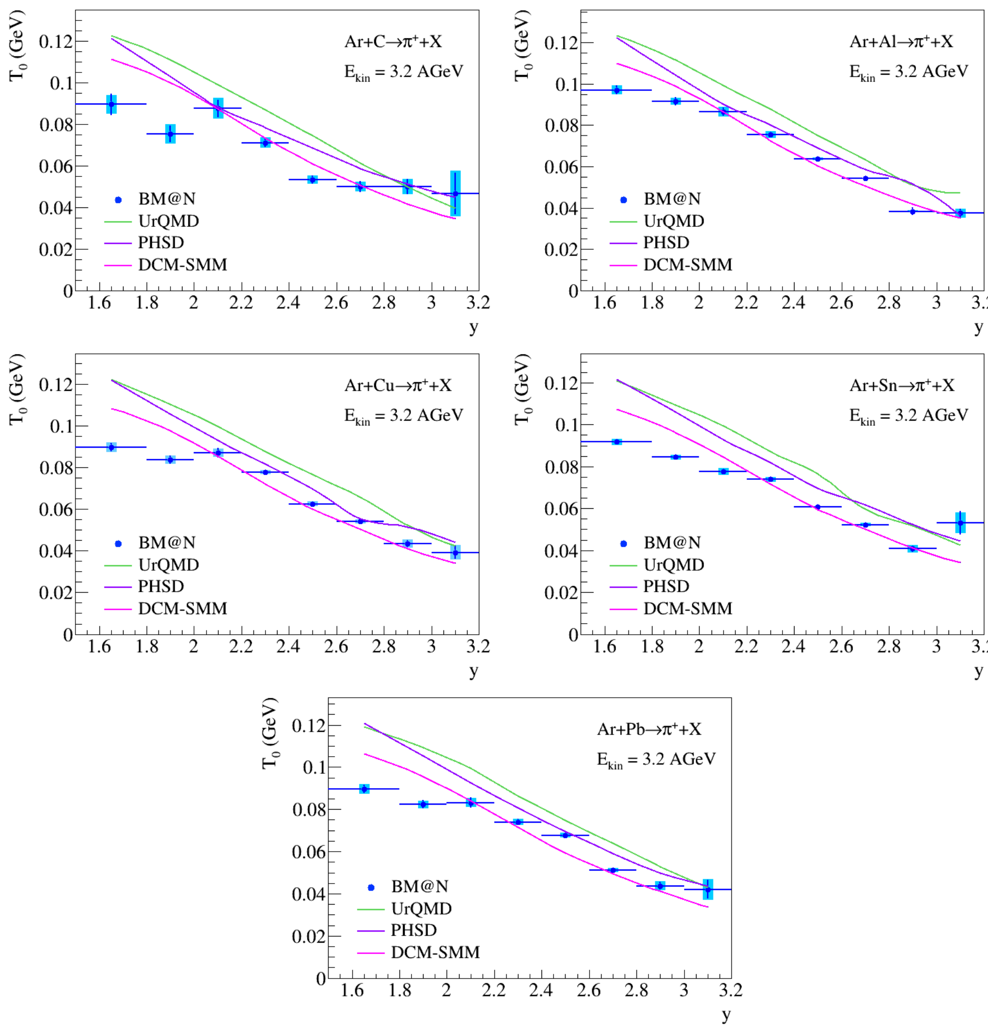

Figure 10: Rapidity y dependence of the inverse slope T_0 extracted from the fits of the π^+ p_T spectra in Ar+C, Al, Cu, Sn, Pb interactions. The error bars represent the statistical errors, the boxes show the systematic errors. The predictions of the DCM-SMM, UrQMD and PHSD models are shown as rose, green and magenta lines.

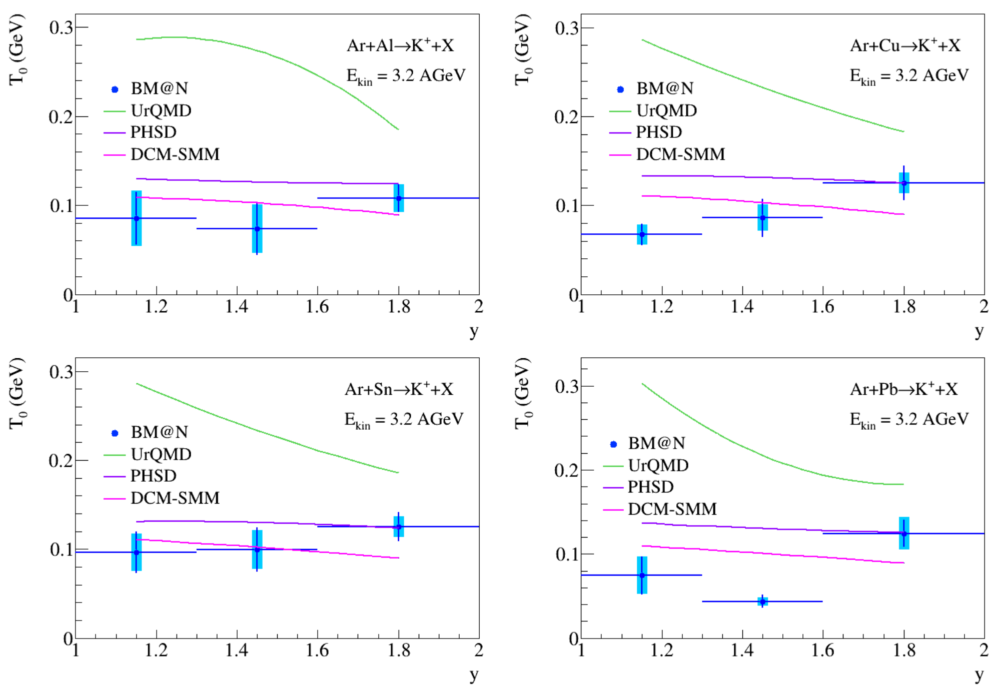

Figure 11: Rapidity y dependence of the inverse slope T_0 extracted from the fits of the K^+ p_T spectra in Ar+Al, Cu, Sn, Pb interactions. The error bars represent the statistical errors, the boxes show the systematic errors. The predictions of the DCM-SMM, UrQMD and PHSD models are shown as rose, green and magenta lines.